

PACS numbers: 42.30.Ms; 42.62.Be; 87.19.xj
DOI: 10.1070/QE2012v042n05ABEH014885

Adaptation of LASCA method for diagnostics of malignant tumours in laboratory animals

S.S. Ulianov, V.N. Laskavy, A.B. Golova, T.I. Polyanina,
O.V. Ulianova, V.A. Feodorova, A.S. Ulianov

Abstract. **The LASCA method is adapted for diagnostics of malignant neoplasms in laboratory animals. Tumours are studied in mice of Balb/c inbred line after inoculation of cells of syngeneic myeloma cell line Sp.2/0–Ag.8. The appropriateness of using the tLASCA method in tumour investigations is substantiated; its advantages in comparison with the sLASCA method are demonstrated. It is found that the most informative characteristic, indicating the presence of a tumour, is the fractal dimension of LASCA images.**

Keywords: *LASCA method, malignant neoplasms, fractal dimension.*

1. Introduction

At present the diagnostics of malignant neoplasms is typically accomplished using the methods of X-ray and fluorescent diagnostics, ultrasound imaging, and tissue biopsy. In studies *in vivo* the problem of particular urgency is to provide an objective measurement of the tumour size and monitoring of growth or regression of the tumour in laboratory animals in the process of cancer therapy. In the present paper the method of laser speckle contrast analysis (LASCA) is used for tumour diagnostics [1, 2]. Earlier this method was used to study cerebral blood flow in a normal state and at different pathologies [3–5], to test new generation of vaccine preparations against particularly dangerous infections [6], and to study hydrodynamic blood microflows in solitary vessels of white rat mesentery [7].

We should particularly mention the use of the methods of speckle-diagnostics in the studies of microcirculation in strongly scattering tissues, to which the cancer tumours belong. Earlier the attempts of using such methods for studying malignant neoplasms were already made [8–13]; however, the practical use of the LASCA method in cancer diagnostics is associated with great difficulties.

Since the monitoring of growth/regression of tumours should be performed in dynamics, i.e., in the process of treatment, the method of diagnostics should be completely noninvasive. First, it means that any damage of the tumour itself and the surrounding tissues must be excluded. If the tumour is localised inside the organism (not at the skin surface), then it is covered with the skin tissues, containing blood vessels. The motion of blood in the latter gives rise to additional speckle dynamics that masks the useful signal from the tumour tissue. The influence of skin blood flow should be eliminated. For example, in studies of cerebral blood flow a fragment of cutaneous covering is removed from the head of a white rat, and after the experiment that lasts 40 minutes the animal is sacrificed. In tumour investigations the use of such traumatic technique is principally impossible, since the measurements are performed multiply during three-four weeks.

Second, the use of any contrast agents is unacceptable, since in combination with the tested new antineoplastic preparations [14] they may exert uncontrollable influence on the process of growth/regression of the neoplasm.

Third, the use of any narcotising preparations is undesirable. Recently the first papers [15] were published on the use of LACA methods for studying cerebral blood flow in laboratory animals, freely moving in the cage. To solve this problem, the miniature measuring unit was fixed at the animal's head. However, this approach is absolutely unacceptable in the case of studying tumours localised in soft tissues. Anaesthetisation, as a rule with Nembutal, is commonly used to eliminate motion activity of a laboratory animal and to fix it at the measuring setup. Multiple administration of narcotising drugs during a few weeks may essentially affect the process of tumour formation; however, at present the combined action of narcotics with tested new antineoplastic biocomposites is absolutely unexplored.

It is worth noting that initially the LASCA method was developed for blood flow studies just in the brain tunics of white rats. In the process of brain probing the laser radiation is scattered by the scull bones, located beyond the brain tissues. The scattering properties of upper layers of skin strongly differ from the scattering characteristics of other biological tissues, particularly, from the properties of bone tissue. Hence LASCA requires adaptation to the problems of malignant tissue diagnostics, as well as detailed approbation under the laboratory conditions.

Solving this problem is the aim of the present paper.

S.S. Ulianov, A.S. Ulianov N.G. Chernyshevsky Saratov State University (National Research University), ul. Astrakhanskaya 83, 410012 Saratov, Russia; e-mail: ulianov@sgu.ru;
V.N. Laskavy, A.B. Golova, T.I. Polyanina Saratov Research Veterinary Institute of Russian Academy of Agricultural Sciences, ul. 53 Strelkovoy Divizii 6, 410028 Saratov, Russia;
O.V.Ulianova N.G. Chernyshevsky Saratov State University (National Research University), ul. Astrakhanskaya 83, 410012 Saratov, Russia; Saratov Research Veterinary Institute of Russian Academy of Agricultural Sciences, ul. 53 Strelkovoy Divizii 6, 410028 Saratov, Russia;
N.I. Vavilov Saratov State Agricultural University, Teatral'naya pl. 1, 410012 Saratov, Russia; e-mail: ulianovaov@mail.ru;
V.A. Feodorova Saratov Scientific and Research Veterinary Institute, Russian Academy for Agricultural Sciences, ul. 53 Strelkovoy Divizii 6, 410028 Saratov, Russia; N.I. Vavilov Saratov State Agricultural University, Teatral'naya pl. 1, 410012 Saratov, Russia;
e-mail: fedorovaav@mail.ru

Received 11 April 2012
Kvantovaya Elektronika **42** (5) 399–404 (2012)
Translated by V.L. Derbov

2. Materials and methods

2.1. Laboratory animals

In the experiments we used 12-week-old white mice of the inbred line Balb/c having the weight 20 g, syngeneic (i.e., genetically identical, or sufficiently identical and immunologically compatible) with respect to myeloma cells Sp.2/0–Ag.8. For control the intact mice of the same line were used. The animals were supplied by the licensed breeding station 'Andreevka' of the Research Centre of Biomedical Technologies, Russian Academy of Medical Sciences (Moscow Region, Solnechnogorsky District, settlement of Andreevka). To study the statistical characteristics of skin by means of coherent microscopy we used outbred white mice.

2.2. Cell culture (plasmacytoma line)

Tumour formation was induced by inoculation of cells of murine plasmacytoma of Sp.2/0–Ag.8 line to inbred mice. To provide formation of a solid (i.e., localised) tumour, 0.5 mL of cell suspension, containing 6×10^5 cells of the mentioned syngeneic myeloma line, was injected intramuscularly. Preliminarily the animals were subjected to intraperitoneal injection of Pristane mineral oil for efficient grafting of tumour cells [16].

2.3. Preparation of outbred mice skin samples for coherent microscopy

In the process of studies it was assumed that the scattering characteristics of outbred mice skin do not differ from similar characteristics of inbred line mice. The outbred mice skin layers were cut horizontally using an MZ-2 freezing microtome (Russia). Each cut skin sample was placed between two cover glasses. The edges of the obtained sandwich structure were hermetically closed with paraffin. Between the experiments the samples were kept in a freezing camera at the temperature –18 °C. It should be noted that the samples may be extremely diverse, which reflects complex structure of skin; sometimes they can contain a fragment of capillary network. The following samples taken from different depth were prepared: 50 μm (cuts from the depth 70, 220, 570, and 1420 μm), 100 μm (from the depth 620 and 1470 μm), 150 μm (depth 720 and 1570 μm) 200 μm (depth 320 and 870 μm), 300 μm (depth 1070 and 1920 μm), and 400 μm (depth 400 and 800 μm).

2.4. Setup for studying the scattering properties of skin

As shown earlier [3], in the LASCA method the optimal ratio of the mean speckle size to the pixel size of the used camera is close to unity. Note, that in visualisation of brain microvessels of laboratory animals the speckle dynamics is observed only in small areas of the registered speckle structure. These areas are localised in space and exactly correspond to the position of the observed solitary microvessels. The rest of the registered speckle structure contains only static speckles. Hence, the mean speckle size can be determined directly from the results of statistical processing of individual realisations of the static speckle-field.

However, in tumour study the situation is absolutely different from the described above. Since the tumour contains extremely large number of microvessels, the registered speckle structure contains only dynamical speckles, which are not localised in the image plane. When using LASCA methods, the acquisition time of an individual frame strongly exceeds the correlation time of the speckle-field intensity fluctuations; therefore, the recorder speckles are time-averaged. The transverse dimension of the averaged speckles does not coincide with the size of statistical speckles. Therefore, from the point of view of adapting LASCA methods to the problems of diagnostics and monitoring of tumour growth, the problem of measuring the mean speckle size appears to be of particular interest.

The *in vitro* observation of biospeckles that arise due to the scattering of coherent light in skin slices was performed by means of Biolam microscope (LOMO, Russia), in which the incoherent white light source was replaced with the GN-5P He–Ne laser (power 5 mW, wavelength $\lambda = 633$ nm). The output Gaussian beam with the diameter 1 mm was transformed into a collimated beam with the diameter that could be varied within the interval from 1 to 7 mm. The collimation was implemented by means of the system, consisting of two parts. The first part of the collimating system was formed by two lenses. The front focal plane of the second lens having the focal length 10 mm and the numerical aperture 0.55 (AL1210-A, S-LAH64 Aspheric Lens, Thorlab, USA) was coincident with the back focal plane of the first lens having the focal length 1.14 mm and the numerical aperture 0.44 (C200TM-B, Thorlab, USA). This part of the collimating system was used to obtain a widened beam with the diameter 7 mm. The second part of the collimating system also consisted of two lenses with the focal length 1.14 mm and numerical aperture 0.44 (C200TM-B, Thorlab, USA) between which in the plane of beam focusing a spatial filter, consisting of a diaphragm with a pinhole 5 μm in diameter (P5S, Thorlab, USA), was installed. All lenses and the spatial filter were mounted in two standard lens tubes (SM05L10, 0,5″ Lens Tube Thorlab, USA) with the iris (D5S, Thorlab, USA) between them. The iris was aimed at matching the diameter of the collimated beam with the size of the fragment of the sample that visually seemed to be most statistically uniform. To control the illumination intensity a rotating attenuator (NDC-100C-4M, Mounted Continuously Variable ND Filter, Thorlab, USA) was installed in front of the collimating system. It was a neutral filter with the optical density, controllable within the range 0–4. The collimated beam was directed onto the studied skin sample by means of a mirror (ME05-M01, Gold, Thorlab, USA).

Speckles were observed directly at the surface of the studied skin sample. For observation the oil immersion 90× objective with the numerical aperture 1.25 (1OMO, Standa, Lithuania) was used. In the field aperture plane a monochrome digital CMOS camera WinCamD (DataRay, USA) having the resolution 1024×1024 pixels was installed, by means of which recording of speckle structures in the image plane of the object was performed. To reduce the noise level in the recorded speckle fields the regime including the averaging over 100 realisations was used. A typical speckle structure, observed under the illumination of a 200-μm-thick skin slice with a collimated laser beam, is shown in Fig. 1a.

For further processing a1D realisation, i.e., one central horizontal line (Fig. 1b), was extracted from the 2D realisation of the speckle field. To suppress the statistical heterogeneity we applied additional smoothing by means of the moving median method. Later this trend was eliminated, after

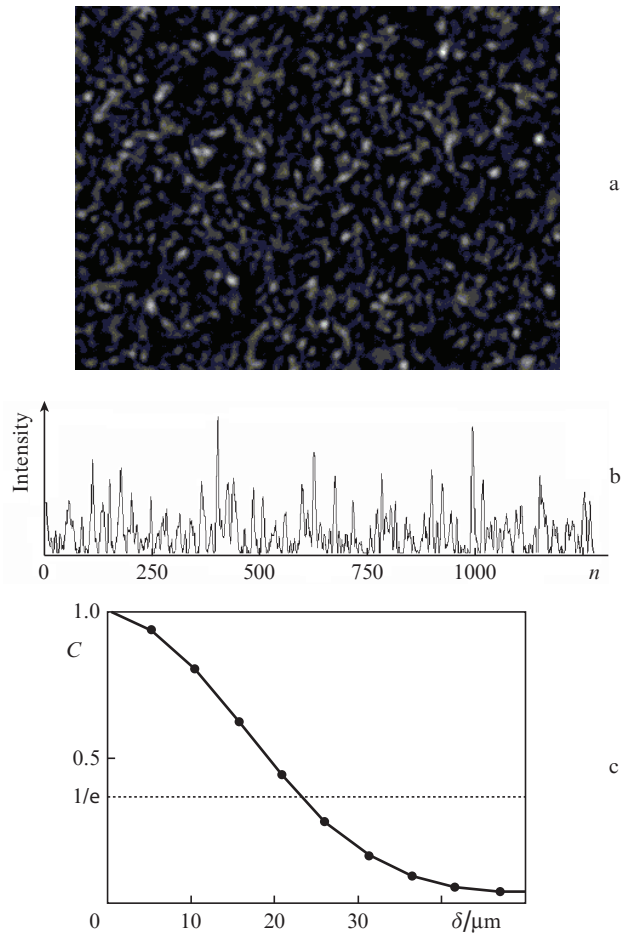

Figure 1. Biospeckles arising under illumination of a skin slice with a collimated laser beam: a fragment of a two-dimensional speckle structure (a) and its one-dimensional realisation (n being the number of a pixel) (b), as well as the normalised transverse correlation function of the scattered field intensity fluctuations (c).

which the spatial correlation function of the speckle field was calculated. The correlation function in the region of small values was interpolated by splines, which provided its calculation with subpixel spatial resolution.

2.5. Setup for study of blood microcirculation using LASCA method

To obtain the LASCA image we used the lens with the focal length 30 mm and the diameter 12.7 mm (AC254-030, Thorlab, USA). The tissues were illuminated at the angle 40° with respect to the normal direction by means of the collimating system, described in Section 2.4. The principle of speckle-field procession using dynamical LASCA method consists in the following. At each point of the dynamical speckle structure the contrast of dynamical speckles is calculated using the formula

$$V = \frac{\sqrt{\langle (I - \langle I \rangle)^2 \rangle}}{\langle I \rangle} = \frac{\sigma_I}{\langle I \rangle}, \qquad (1)$$

where I is the instantaneous intensity of dynamical biospeckles; σ_I is the standard deviation of intensity fluctuations; the angle brackets mean averaging over time. To obtain the image of the visualised tissues we used averaging over 500 registered frames of the dynamical speckle field, recorded using the monochrome CMOS camera Phoenix 1280 USB DC (MuTech, USA). The visual field was as large as 11×11 mm, the magnification of the optical system was equal to 0.46, the spatial resolution in the object plane was 11.3 μm.

3. Study of speckle formation processes inside a skin layer of outbred mice

If the skin slice is thin enough, then the measurement of the mean speckle size can be performed directly using the transverse correlation function of the scattered field intensity fluctuations. The speckle size is equal to twice the value of the correlation length. A characteristic example of correlation function is presented in Fig. 1c. If the sample thickness exceeds 100 μm, the speckle size in the observation plane becomes smaller than the camera pixel size. Direct measurement of the mean speckle size in this case becomes impossible. This value may be estimated explicitly from the speckle contrast. As known, the contrast of fully developed speckles is equal to unity. If the scattered light is fully depolarised, the contrast of speckles reduces to 0.7 [17]. As follows from the central limit theorem [18], if the speckles are integrated by the photodetector aperture (in the present case, by an individual pixel of the CMOS camera), then the speckle contrast is reduced by N times more, where N is the mean number of speckles occurring at the photodetector (in the present case, at an individual pixel of the CMOS camera). Therefore, given the speckle contrast and the camera pixel size, one can estimate the mean speckle size. The contrast values for speckles (scattered from the skin and adjacent fatty tissue and muscle) as a function of the layer thickness and location depth are presented in Table 1.

Table 1. Speckle contrast depending on the tissue slice thickness and the depth of its location in intact mice.

Depth/μm	Thickness/μm				
	100	150	200	300	400
150	0.22	0.21	0.27	0.27	0.21
~200	0.28	0.29	0.34	0.29	0.24
300–400	0.23	0.22	0.21	0.21	0.34
500–1000	0.14	0.16	0.23	0.3	0.22
1300–1500	0.22	0.19	0.24	0.2	0.27

As seen from the table, the speckle contrast measured with the CMOS camera is relatively low and lies in the range 0.14–0.34. The contrast measurements allow the following conclusion: the speckles, produced in the murine skin tissues, possess very small dimensions, which in the upper layers of epidermis fall within the range $(1.53–3)\lambda$. For the thickness of the skin sample (with adjacent tissues) of 200–300 μm the speckle size tends to λ.

This conclusion is extremely important from the point of view of adapting the LASCA method to the problems of neoplasm diagnostics. As already mentioned, two main modifications of the LASCA method exist. The first modification (sLASCA) is based on the analysis of an individual realisation of static speckles [19, 20]. In this case the entire realisation of the speckle field is divided into small areas, as a rule, each including 5×5 or 7×7 pixels. For each of the selected small areas the local value of static speckle contrast is calculated, after which the LASCA image is constructed. The second approach (tLASCA) is based on using Eqn (1). Detailed com-

parison of both approaches to the speckle processing is presented in [4].

The studies carried out show that in the case of tumour diagnostics the probing is performed using spatially incoherent light. The contrast of static speckles in this case will tend to zero. The use of preliminary statistical processing of speckle fields, based on the interpolation by *B*-splines, or specific methods of forced contrast enhancement (these methods are referred as rLASCA [21] and eLASCA [22, 23], respectively) allows some improvement of the LASCA images. However, keeping in mind that the contrast of dynamical speckles (unlike the contrast of static ones) does not change as a result of speckle integration by the camera pixel aperture, in tumour diagnostics it is reasonable to use the second modification of LASCA method, namely, the tLASCA, based on processing of dynamical speckles.

4. Adaptation of LASCA method to biomodels syngeneic to malignant tumours

4.1. Animal motion compensation

As already mentioned, in the experiments the laboratory animals were not narcotised. They were firmly fixed at the setup by the aid of cotton cords 1 mm in diameter. However, such fixation method does not allow full elimination of animal motion, caused by the muscular activity and breathing.

To increase the sensitivity of the method, the algorithm of dynamical image processing was substantially modified. At the first stage of the processing a two-dimensional trend was extracted in two successive speckle field images. Then a two-dimensional cross-correlation function between the realisations of two trends was calculated. This is a feature different from the algorithm [5, 7], where the correlation is calculated between high-frequency components of speckle structure with the trend eliminated. The position of the cross-correlation function maximum allows high-precision determination of the relative displacement of images. At the next stage the correction of speckle-field image displacements, caused by breathing and motional activity of the laboratory animal, was carried out.

The trajectory of the animal motion in the process of measurements possesses extremely complex chaotic behaviour. An example of such trajectory is shown in Fig. 2. It is seen that the displacement of the animal may be large enough and reaches 2 mm, which is 1/7 of the entire field of view.

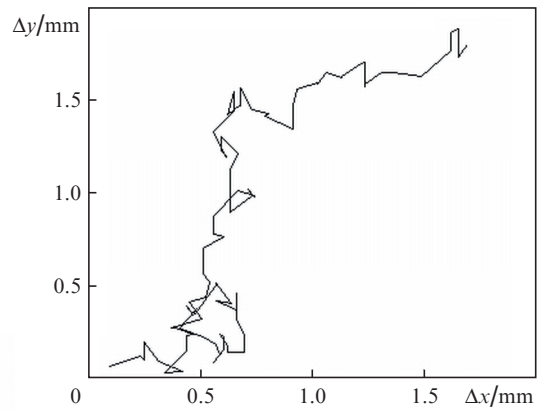

Figure 2. Animal motion trajectory (Δx, Δy are the displacements of the studied object along the coordinate axes).

4.2. Elimination of skin blood flow influence

The motion of blood in skin causes the most intense dynamics of speckles and is the main source of measurement errors. To suppress the biospeckles dynamics caused by light scattering in the microcirculatory network, an additional circular glass window was used having the thickness 2.1 mm and the diameter 14 mm, made of a fragment of the holographic plate PG-3, from which the emulsion layer was previously removed. Under the excess pressure, exerted by the glass window onto the skin surface, the intensity of blood microcirculation and blood filling are noticeably reduced. Visually this is expressed in the change of colour (whitening) of the cutaneous covering.

As known, the use of agents causing optical clearing may significantly change the scattering properties of biotissues [24]. During the experimental studies such agents as petrolatum and polyethylene glycol-400 were applied to the skin of intact mice. However, as shown by the results of the experiments described below, the administration of these agents has absolutely no effect on the structure of LASCA images, although, of course, it must reduce the multiplicity of scattering in the unmovable structures of skin. The coincidence of LASCA images, obtained before and after the optical clearing (see Section 5), implicitly evidences in favour of considerable reduction of skin blood flow due to skin compression.

4.3. Analysis of contrast and fractal dimension of LASCA images

Fractal structures [25] often occur in nature and are studied in numerous fields of research. The fractals occurring in optics [26] are observed in the formation of speckle structures that arise due to light scattering in randomly-inhomogeneous media or to diffraction from rough surfaces. The diffraction patterns, arising in the process of scattering of coherent light in objects of biological origin, are commonly referred as biospeckles [27]. In analogy with this, the optical fractals, produced by diffraction of radiation in biotissues, became to be referred as biofractal images [28] or simply biofractals [29]. In recent years the analysis of fractal structures has found application in solving various problems in biology and medicine. The spectrum of these applications is extremely wide: from early diagnostics of oncological diseases to revealing the tendency to schizophrenia in patients [3–35].

To make the developed method of neoplasm diagnostics more informative, in the present paper, besides measuring the mean spatial contrast of the observed LASCA images, an attempt was made to determine their fractal dimensions (for both intact tissues and those with tumour). The fractal dimensions of the obtained speckle structures were calculated using the covering method. In more detail this algorithm in application to biospeckles is described in [36, 37].

5. Application of LASCA method to the visualisation of solid tumours

The first signs of a tumour (slight swelling with the size nearly 5×5 mm at the site of the injection of myeloma cells) appeared in biomodels on the seventh day after the inoculation. The visualisation of the tumour using the LASCA method was

performed on the 12th day after inoculation of cells of syngeneic myeloma line Sp.2/0–Ag.8 (the tumour size 20 × 20 mm).

The spatial distribution of speckle contrast in the image plane reflects the structure and spatial localisation of deeply deposited tissues of malignant neoplasms. The images of averaged speckles and the spatial distribution of root-mean-square deviation of temporary intensity fluctuations are less informative and reflect, in the first place, the surface irregularities of the studied animal skin, rather than the localisation of microvessels in the capillary network of the tumour. Being absolutely non-informative, these images are not presented here.

In Figs 3a and b the fragments of the LASCA image of the intact animal tissues are shown before and after optical clearing. Naturally, these images could be displaced with respect to each other, since the animal was extracted from the measurement setup for applying the clearing agents. However, as already mentioned above, the images are rather similar in statistical characteristics, possessing close values of contrast and fractal dimensions.

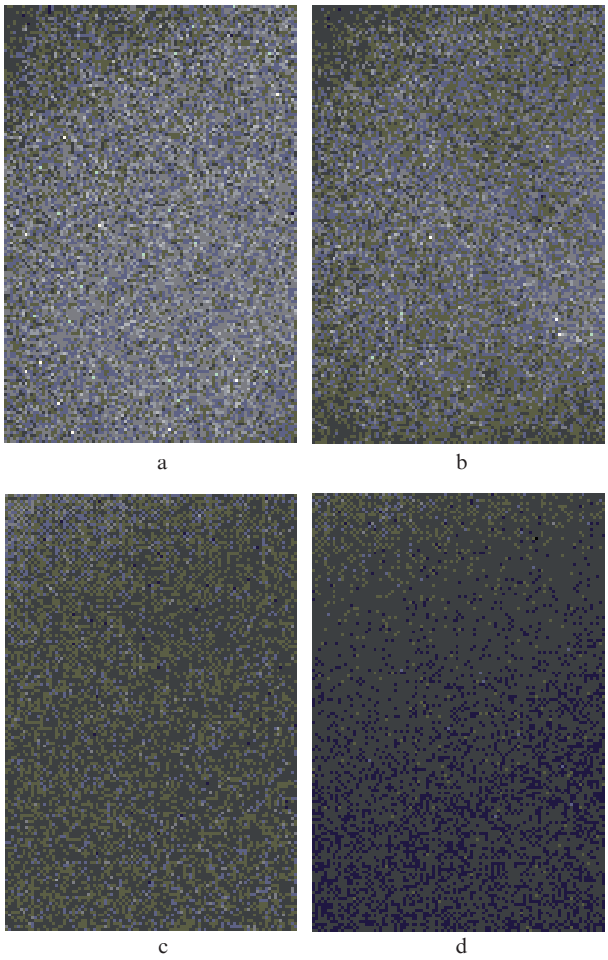

Figure 3. Fragments of LASCA images of intact laboratory animal tissues before (a) and after (b) optical clearing, as well as two images of animal tissues with myeloma (without optical clearing), (c) and (d).

As an example, in Figs 3c and d two LASCA images of animal tissue with mature tumour are presented. Significant difference between the LASCA images of intact animal tissues and those of tumour tissues are seen absolutely clear.

Totally 32 LASCA images obtained in the control (intact tissue) and pathology (tumour) groups were analysed. The analysis of these observations allows the following conclusions.

(i) The testing of the nonparametric hypothesis about the distribution law shows that such indicators as the contrast and the fractal dimension obey the normal distribution law (in norm and pathology) at the significance level $\alpha = 0.05$.

(ii) The problem of comparing mean values of two normally distributed statistical ensembles with the variances being unknown and unequal (by sample estimates) is known as the Behrens–Fisher problem. The solution of this problem in application to the comparison of mean values of the fractal dimensions and the contrast of LASCA images (in norm and pathology) was implemented on the base of checking the hypothesis by means of the Cochran–Cox criterion, as well as Satterwhite and Welch criteria [38]. (The hypothesis about the equality of mean values of fractal dimensions of the LASCA images, recorded in norm and in the case of a malignant tumour, is rejected.) In other words, the hypothesis testing indicates the presence of valuable and significant differences in the values of the fractal dimension of LASCA images of intact tissues and those with myeloma. The hypothesis of equal mean values of LASCA image contrast values, recorded in norm and pathology, is accepted at the significance level $\alpha = 0.05$. This means that the contrast of LASCA image of intact tissue, in fact, does not differ from that of the tissue with myeloma. Therefore, contrast is a low-informative parameter, and its use in the tumour diagnostics is not reasonable.

(iii) The statistical estimation [39] of the confidence interval of the fractal dimension mean value was carried out. It is found that with 95% probability the mean value of the LASCA image fractal dimension, obtained for skin of intact animals, lies within a very narrow interval of [0.097; 0.098], while in the case of malignant neoplasms this interval is [0.169; 0.173]. Therefore, it is reliably established that the fractal dimension of LASCA images, recorded from myeloma tumour, increases by 75% as compared with control, the possible measurement error not exceeding ±1.3%.

Thus, in future the proposed method of diagnostics may be used for objective control in optimisation of prevention schemes and elaborating individual regimes of administering antineoplastic drugs under testing [14] in the treatment of oncologic diseases.

References

1. Briers J.D., Webster S. *J. Biomed. Opt*., **1** (2), 174 (1996).
2. Briers D. *J. Physiol. Meas*., **22**, R35 (2001).
3. Dunn A.K., Bolay H., Moskowitz M.A., Boas D.A. *J. Cerebral Blood Flow Metabolism*., **21**, 195 (2001).
4. Li P., Ni S., Zhang L., Zeng S., Luo Q. *Opt. Lett*., **31**, 1824 (2006).
5. Sini M.S., Linsely J.A. *Proc on Signal Processing, Communication, Computing and Networking Technol*. (Piscataway, New Jersey, USA, 2011, ICSCCN-2011) p. 207.
6. Ulianova O.V., Ulianov S.S., Pengcheng Li, Qingming Luo. *Kvantovaya Elektron*., **41** (4), 340 (2011) [*Quantum Electron*., **41** (4), 340 (2011)].
7. Ulyanov S., Ganilova Y., Zhu D., Qiu J., Li P., Ulianova O., Luo Q. *Europhys. Lett*., **82** (1), 18005-p1 (2008).
8. Draijer M., Hondebrink E., Ton van Leeuwen, Steenbergen W. *Lasers Med Sci*., **21** (4), 208 (2006).
9. Miao P., Li N., Thakor N.V., Tong S. *Opt. Express*, **18** (1), 218 (2010).

10. Zhu D., Lu W., Weng Y., Cui H., Luo Q. *Appl. Opt*., **46** (10), 1911 (2007).
11. Kruijt B., de Bruijn H. S., van der Ploeg-van den Heuvel A., Sterenborg H.J., Robinson D.J. *Lasers Med Sci*., **21** (4), 208 (2006).
12. Yu P., Peng L., Mustata M. *Opt. Lett*., **29**, 68 (2004).
13. Kalchenko V., Madar-Balakirski N., Kuznetsov Y., Meglinski I., Harmelin A. *Proc. SPIE–OSA Biomed. Opt.*, **8090**, 809007 (2011).
14. Tishkin S.M., Laskavyj V.N. *Cytostatic Composition*. European Patent EP20090814148; US Patent US 2009/0203800 A1.
15. Miao P., Lu H., Liu Q., Li Y., Tong S. *J Biomed. Opt*., **16** (8), 086011 (2011).
16. Feodorova V.A., Gromova O.V., Devdariani Z.L., Dzhaparidze M.N., Teryoshkina N.Y. *J. Med. Microbiol*., **6**, 499 (2001).
17. Goodman J. *Statistical Optics* (New York: Wiley, 1985; Moscow: Mir, 1985).
18. Bendat J.S., Piersol A.G. *Random Data: Analysis and Measurement Procedures* (New York: John Wiley & Sons, 2000; Moscow: Mir, 1989).
19. Luo Q., Qiu J., Li P., in *Advanced Optical Flow Cytometry: Methods and Disease Diagnoses* (Berlin: Wiley-VCH Verlag GmbH & Co, 2011) p. 605.
20. Le T.M., Paul J.S., Ong S.H., in *Computational Biology: Issues and Applications in Oncology (Applied Bioinformatics and Biostatistics in Cancer Research)* (New York–Dordrecht–Heidelberg–London: Springer, 2009) p. 243.
21. Miao P., Rege A., Li N., Thakor N., Tong S. *IEEE Trans Biomed Eng*., **57** (5), 1152 (2010).
22. Yu J., Miao P., Li M., Qiu Y., Zhu Y., Tong S. *Proc. of the Intern. Conf. IEEE Engineering in Medicine and Biology Society* (Washington, 2008, p. 3743).
23. Miao P., Li M., Fontenelle H., Bezerianos A., Qiu Y., Zhu Y., Tong S. *IEEE Transac. Biomed. Eng*., **56** (4), 1127 (2009).
24. Genina E.A., Bashkatov A.N., Tuchin V.V. *Expert Rev. Med. Devices*, **7** (6), 825 (2010).
25. Mandelbrot B. *The Fractal Geometry of Nature* (San Francisco: W.H.Freeman and Co., 1982).
26. Uozumi J., Ibrahim M., Asakura T. *Opt. Commun*., **156**, 350 (1998).
27. Aizu Y., Asakura T., in *Optics and Lasers in Biomedicine and Culture, Optics Within Life Sciences (OWLS V)* (Berlin: Springer, 2000) p. 297.
28. Angelsky O.V., Ushenko A.G., Burkovets D.N., Pishak O.V., Ushenko Yu.A., Pishak V.P. *Proc. SPIE Int. Soc. Opt. Eng*., **4829**, 188 (2003).
29. Ushenko Yu.A., Kuritscin A.N. *Proc. SPIE Int. Soc. Opt. Eng*., **4242**, 233 (2001).
30. Einstein A.J., Wu H.S., Gil J. *Phys. Rev. Lett*., **80**, 397 (1998).
31. Bauer W. *Heavy Ion Phys*., **14**, 39 (2001).
32. Hunter M., Backman V., Popescu G., Kalashnikov M., Boone C.W., Wax A., Venkatesh G., Badizadegan K., Stoner G.D., Feld M.S. *Phys. Rev. Lett*., **97**, 138102 (2006).
33. Sboner A., Bauer P., Zumiani G., Eccher C., Blanzieri E., Forti S., Cristofolini M. *Skin Research and Technology*, **10** (3), 184 (2004).
34. Kelloff G.J., Sullivan D.C., Baker H., Wax A. *Cancer Biomarkers*, **3** (1), 1 (2007).
35. Brown W.J., Pyhtila J.W., Terry N.G., Chalut K.J., D'Amico T.A., Sporn T.A., Obando J.V., Wax A. *IEEE J. Sel. Top. Quantum Electron*., **14**, 88 (2008).
36. Ulianov A.S., Lyapina A.M., Ulianova O.V., Fedorova V.A., Ulianov S.S. *Kvantovaya Elektron*., **41** (4), 349 (2011) [*Quantum Electron*., **41** (4), 349 (2011)]
37. Ulianov A.S. *Kvantovaya Elektron*., **38** (6), 557 (2008) [*Quantum Electron*., **38** (6), 557 (2008)].
38. Kobzar' A.I. *Prikladnaya matematicheskaya statistika* (Applied Mathematical Statistics) (Moscow: Fizmatlit, 2008).
39. Chap T. *Introductory Biostatistics* (New Jersey: John Wiley & Sons Inc. Hoboken, 2003).